EMPIRICAL BAYES ESTIMATOR FOR ENDOCARDIAL EDGE DETECTION IN 3D+T ECHOCARDIOGRAPHY

Engin Dikici[1], *Fredrik Orderud*[2], *Bo Henry Lindqvist*[1]

[1]Norwegian University of Science and Technology, Trondheim, Norway
[2]GE Vingmed Ultrasound, Oslo, Norway

ABSTRACT

This paper presents an empirical Bayes (EB) estimator for detection of endocardial edges in 3D+T echocardiography recordings. A maximum likelihood (ML) edge detector, proposed in a previous study, combines the responses of multiple edge detectors to improve the detection accuracy. We aim to further extend this approach with the use of contextual priors, that gives the probabilistic distribution of correct (yet unknown) endocardial edge positions. For training, a ML model that gives an optimal linear combination of multiple endocardial edge detectors is learned from a pre-segmented dataset. For a given test data, (1) ML edges are estimated using the learned ML model, (2) a conceptual prior is derived using the ML edge estimations in an empirical fashion, and (3) ML estimates and the conceptual prior are fused to produce empirical Bayes endocardial edge estimates. Comparative analyses show that EB reduces the mean square endocardial surface error with respect to ML estimations. This is due to the Stein effect that briefly asserts that the expected mean square error of the ML estimations should be reduced with the use of empirically-derived prior information.

Index Terms— Empirical Bayes, Stein Effect, 3D+T Echocardiography Tracking, Ensemble Methods.

1. INTRODUCTION

This paper considers the problem of endocardial border detection in 3D+T echocardigraphy recordings. This is a challenging task due to problems including (1) speckle noise, (2) shadowing that can result in missing boundaries, and (3) the existence of intra-cavity structures such as chordae tendineae, papillary muscles and valves [1]. Furthermore, real time, or nearly real time, detection of endocardial borders might be necessary during invasive procedures and intensive care.

A Kalman tracking framework can be employed for rapid and model based detection of endocardial borders in 3D+T recordings. The approach utilizes a sequential prediction and update strategy, where surface deformations are first predicted by a kinematic model, followed by an update step based on information provided by image measurements. Maximum gradient (MG) [2], step criterion (STEP) [3], local-phase [4] and max flow/min cut (MFMC) [5] edge detectors were previously employed for the image measurement stage of the Kalman tracking framework. In [6], a maximum likelihood (ML) edge detector that combines the responses of multiple base detectors (e.g. MG, STEP and MFMC) via learned statistical inferences was introduced. The method was shown to be more accurate than the base detectors, however it had 2 major limitations: (1) the edge detectors were assumed to be uncorrelated, and (2) statistical properties of the edge detectors were marginalized to the endocardial surface. More recently, the shortcomings of [6] were addressed by an improved ML method employing both cardiac cycle and endocardial surface position dependent statistics [7].

In this paper, we further extend the ML endocardial edge detector, proposed in [7], by incorporating contextual priors giving the probabilistic distribution of endocardial edges around a surface model. A pre-segmented training dataset is used for learning a ML model, giving the optimal base detector weights for each cardiac cycle and endocardial surface position. For testing, ML edges are first estimated using the ML model. Next, the ML estimates are utilized to empirically compute Gaussian contextual prior parameters. Finally, the ML estimates are combined with the contextual prior to produce empirical Bayes (EB) estimations for the endocardial edge positions (see Figure 1). The effectiveness of the introduced method is represented via comparative analyses among MG, STEP, MFMC, ML and EB.

2. METHODS

2.1. Kalman Tracking Framework

The tracking framework is built around a deformable subdivision model parametrized by a set of control vertices with associated displacement direction vectors. Model deformations are handled by a composite transform, where local shape deformations are obtained by moving control vertices in the subdivision model together with a global transformation that translates, rotates and scales the model as a whole. A manually constructed Doo-Sabin surface is used as a template for representing the endocardial borders, where the model control vertices are allowed to move in the surface normal direction

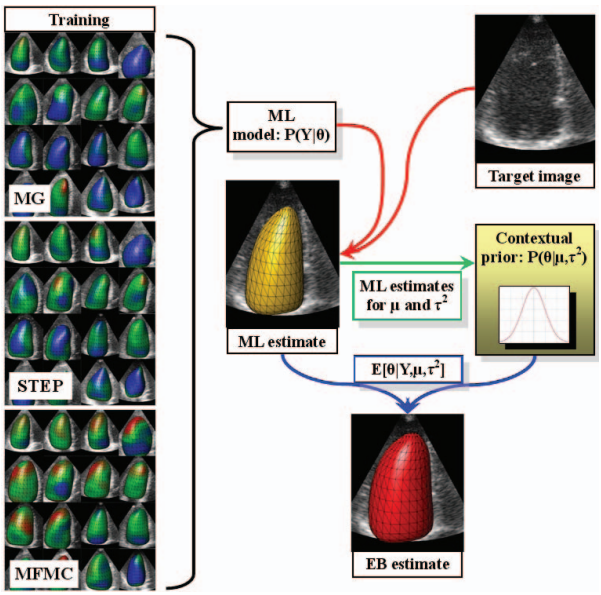


Fig. 1. Overview of the proposed approach. Training stage produces a ML model. Next, the ML model is used for finding a ML estimate that is also utilized to derive a contextual prior. Finally, the ML estimate and the contextual model are combined to produce an EB estimate.

to alter the shape.

The tracking framework consists of five separate stages, namely (1) state prediction, (2) evaluation of tracking model, (3) edge measurements, (4) measurement assimilation, and (5) measurement update [8].

Endocardial edge detection methods are employed during the *edge measurements* stage of the framework. The edge detection is performed by first extracting N 1D intensity profiles centered around the surface points, which are spread evenly across the endocardial surface model. The intensity profiles are oriented in the surface normal directions. MG, STEP and MFMC edge detectors, also referred as the base detectors, define different intensity profile processing schemes to estimate endocardial edge positions [7]. ML and EB edge detectors, combining the responses of these base detectors, are described in the following subsections.

2.2. Maximum Likelihood Edge Detector (ML)

The estimation accuracies of MG, STEP and MFMC vary depending on both endocardial surface and cardiac cycle positions [5, 7]. As an example, MFMC might be the most successful method for the apical inferior region, while performing poor for the mid inferior region at end diastole (ED). On the other hand, STEP might outperform the other methods for both the apical inferior and mid inferior regions at end systole (ES). The responses of multiple edge detectors can be combined using a statistical learning approach for generating better edge estimates; the confidences of the detectors for a given spatial and temporal position determine their weights.

The system can be described for the i^{th} intensity profile at cardiac cycle position $\zeta \in [0:ES,\, 1:ED]$ using a general linear model as:

$$\mathbf{s_{i,\zeta}} = \mathbf{1}\theta_{\mathbf{i},\zeta} + \mathbf{b_{i,\zeta}} + \mathbf{w_{i,\zeta}}, \tag{1}$$

where $\theta_{\mathbf{i},\zeta}$ is the unknown edge position (scalar valued), $\mathbf{s_{i,\zeta}}$ is the measurement vector of the edge detectors, $\mathbf{b_{i,\zeta}} = \left[Bias_{i,\zeta}^{MG},\, Bias_{i,\zeta}^{STEP},\, Bias_{i,\zeta}^{MFMC}\right]^T$ is the learned bias vector for the i^{th} intensity profile at time ζ, and $\mathbf{w_{i,\zeta}} = \left[w_{ij}^{MG},\, w_{ij}^{STEP},\, w_{ij}^{MFMC}\right]^T$ is the noise vector with a learned Gaussian probability distribution function (PDF) $N\left(0,\, C_{i,\zeta}\right)$. Note that $C_{i,\zeta}$ is a 3×3 symmetric matrix holding the error covariances between the base detectors (e.g. $C_{i,\zeta}\left(1,1\right)$ holds the error variance of MG detector's edge estimations, and $C_{i,\zeta}\left(2,3\right)$ holds the error covariance between STEP and MFMC detectors' edge estimations for the i^{th} intensity profile at ζ). The bias vector can be merged with the measurement vector giving,

$$\mathbf{y_{i,\zeta}} = \mathbf{1}\theta_{\mathbf{i},\zeta} + \mathbf{w}_{i,\zeta}. \tag{2}$$

Maximum likelihood estimator of $\theta_{i,\zeta}$ can be derived as [7]:

$$\hat{\theta}_{i,\zeta}^{ML} = \frac{\mathbf{1}^T C_{i,\zeta}^{-1}}{\mathbf{1}^T C_{i,\zeta}^{-1}\mathbf{1}}\mathbf{y_{i,\zeta}}. \tag{3}$$

$\hat{\theta}_{i,\zeta}^{ML}$ is an unbiased estimator with the variance of $\sigma_{i,\zeta}^2 = \left(\mathbf{1^T} C_{i,\zeta}^{-1}\mathbf{1}\right)^{-1}$. The estimator variance can be utilized as the measurement noise in the Kalman filter. ML endocardial edge estimations for the model at ζ are given as,

$$\hat{\theta}_{i,\zeta}^{ML} \sim N\left(\theta_{\mathbf{i},\zeta},\, \sigma_{i,\zeta}^2\right), \qquad i = 1, \ldots, N. \tag{4}$$

2.3. Empirical Bayes Edge Detector (EB)

$\hat{\theta}_{i,\zeta}^{ML}$ is both the best linear unbiased and maximum likelihood estimator for $\theta_{i,\zeta}$, which might seem enough to declare $\hat{\theta}_{i,\zeta}^{ML}$ as an optimal detector for a given base detector set. However, if all the base detectors are producing highly correlated and wrong results for some parts of the endocardium, it becomes obvious that a better estimator should benefit from an additional bias term occasionally. Empirical Bayes estimator (1) uses a contextual prior model giving the PDF of the endocardial edge displacements, (2) and refines the ML estimations with this prior model to produce biased estimations. The prior model helps pulling low-confidence-inaccurate endocardial edge estimations towards a prior distribution mean, which eventually lowers the estimation mean square error.

Let us make the Bayesian assumption that the contextual prior has a Gaussian PDF given as,

$$\theta_{\mathbf{i},\zeta} \sim N\left(\mu_\zeta, \tau_\zeta^2\right), \qquad i = 1, \ldots, N. \tag{5}$$

The Bayes estimate for $\theta_{\mathbf{i},\zeta}$, which is the expected value of the posterior distribution $p\left(\theta_{i,\zeta} | \, \hat{\theta}_{1,\zeta}^{ML} \ldots \hat{\theta}_{N,\zeta}^{ML}\right)$, is given by,

$$\hat{\theta}_{i,\zeta}^{Bayes} = \left(\frac{\sigma_{i,\zeta}^2}{\sigma_{i,\zeta}^2 + \tau_\zeta^2}\right)\mu_\zeta + \left(\frac{\tau_\zeta^2}{\sigma_{i,\zeta}^2 + \tau_\zeta^2}\right)\hat{\theta}_{i,\zeta}^{ML}. \tag{6}$$

$\hat{\theta}_{i,\zeta}^{Bayes}$is the weighted average of μ_ζ and $\hat{\theta}_{i,\zeta}^{ML}$; the weights used in the weighted average depend on the relative sizes of $\sigma_{i,\zeta}^2$ and τ_ζ^2. Hence the confidences of $\hat{\theta}_{i,\zeta}^{ML}$ and μ_ζ determine their weights. More explicitly, the ML estimations are pulled towards a contextual prior mean μ_ζ with rates determined by their confidences.

The empirical Bayes approach agrees with the Bayes model, and estimates the unknown prior distribution parameters, μ_ζ and τ_ζ^2, from the data [9]. For this estimation task, it uses the marginal distributions of $\hat{\theta}_{i,\zeta}^{ML}$, represented as $m\left(\hat{\theta}_{i,\zeta}^{ML}\right)$. A standard calculation shows that,

$$m\left(\hat{\theta}_{i,\zeta}^{ML}\right) \sim N\left(\mu_\zeta, \sigma_{i,\zeta}^2 + \tau_\zeta^2\right), \qquad i = 1, \ldots, N. \tag{7}$$

The joint marginal distribution of all $\hat{\theta}_{i,\zeta}^{ML}$ is hence given by,

$$m\left(\hat{\theta}_\zeta^{ML}\right) = \prod_{i=1}^{N} \frac{1}{\sqrt{2\pi\left(\sigma_{i,\zeta}^2 + \tau_\zeta^2\right)}} e^{\frac{-\left(\hat{\theta}_{i,\zeta}^{ML} - \mu_\zeta\right)^2}{2\left(\sigma_{i,\zeta}^2 + \tau_\zeta^2\right)}}. \tag{8}$$

Maximum likelihood estimators for μ_ζ and τ_ζ^2 can be found by maximizing the log of this function, solving,

$$\frac{\partial \log\left(m\left(\hat{\theta}_\zeta^{ML}\right)\right)}{\partial \mu_\zeta} = \frac{\partial \log\left(m\left(\hat{\theta}_\zeta^{ML}\right)\right)}{\partial \tau_\zeta^2} = 0, \tag{9}$$

to give the estimates $\hat{\mu}_\zeta$ and $\hat{\tau}_\zeta^2$. Note that $\hat{\mu}_\zeta$ and $\hat{\tau}_\zeta^2$ are asymptotically efficient estimations for μ_ζ and τ_ζ^2 [10]. The Empirical Bayes estimate is found by placing these estimated prior distribution parameters into Equation 6 by,

$$\hat{\theta}_{i,\zeta}^{EB} = \left(\frac{\sigma_{i,\zeta}^2}{\sigma_{i,\zeta}^2 + \hat{\tau}_\zeta^2}\right)\hat{\mu}_\zeta + \left(\frac{\hat{\tau}_\zeta^2}{\sigma_{i,\zeta}^2 + \hat{\tau}_\zeta^2}\right)\hat{\theta}_{i,\zeta}^{ML}. \tag{10}$$

$\hat{\theta}_{i,\zeta}^{EB}$ uses all $\hat{\theta}_{i,\zeta}^{ML}$ for detecting the endocardial edges taking the advantage of the *Stein effect*. The Stein effect briefly asserts that the estimation accuracy can be improved by using the information coming from the full model. It can be shown that for $N \geq 4$,

$$E\left[\sum_{i=1}^{N}\left(\theta_{i,\zeta} - \hat{\theta}_{i,\zeta}^{EB}\right)^2\right] < E\left[\sum_{i=1}^{N}\left(\theta_{i,\zeta} - \hat{\theta}_{i,\zeta}^{ML}\right)^2\right], \tag{11}$$

where the expectation is over the distribution of $\hat{\theta}_{i,\zeta}^{ML}$ given $\theta_{i,\zeta}$ [9]. Therefore, a lower mean square surface error is expected for the empirical Bayes estimator compared with the maximum likelihood estimator theoretically.

	MG	STEP	MFMC	ML	EB
ED	15.53	11.05	8.90	7.00	6.11
ES	17.22	7.27	10.31	8.21	7.44

Table 1. Squared surface point errors (in mm^2) for the Kalman tracking framework using MG, STEP, MFMC, ML, EB methods for ED and ES frames.

3. RESULTS

18 apical 3D echocardiography recordings were acquired using a Vivid 7 ultrasound scanner (GE Vingmed Ultrasound, Norway) and a matrix array transducer. The endocardial border segmentation of the recordings were performed by a medical expert using a semi-automatic segmentation tool (4D AutoLVQ, GE Vingmed Ultrasound, Norway).

A 3-fold cross validation (CV) was applied for validation of the ML and EB edge detectors. For each testing fold, the other 2 folds were used for learning a ML model at the ED and ES frames. The ML model included bias, covariance and corresponding ML weights at 528 evenly distributed endocardial surface positions. The learned model was later interpolated between ED and ES through the cardiac cycle using linear interpolation (see Figure 2). For testing, (1) ML and EB detectors were used in connection to the Kalman tracking framework with the learned ML model, (2) *squared surface point errors (SSPE)* giving the average squared distances between the estimated and ground truth surface points were computed, and (3) SSPE measurements of the folds were averaged to find final statistics. SSPE based evaluation was performed, since the objective of the study is to lower the mean square estimation error by taking advantage of the Stein effect. SSPE of STEP, MFMC and MG methods were also computed using all 18 recordings (see Table 1).

In the Kalman tracking framework, a handcrafted Doo-Sabin endocardial model consisting of 20 control points was used as LV model [8]. Edge measurements were performed in 528 intensity profiles distributed evenly across the endocardial surface. Each profile consisted of 30 samples, spaced $1\ mm$ apart. The tracking framework is implemented in C++,

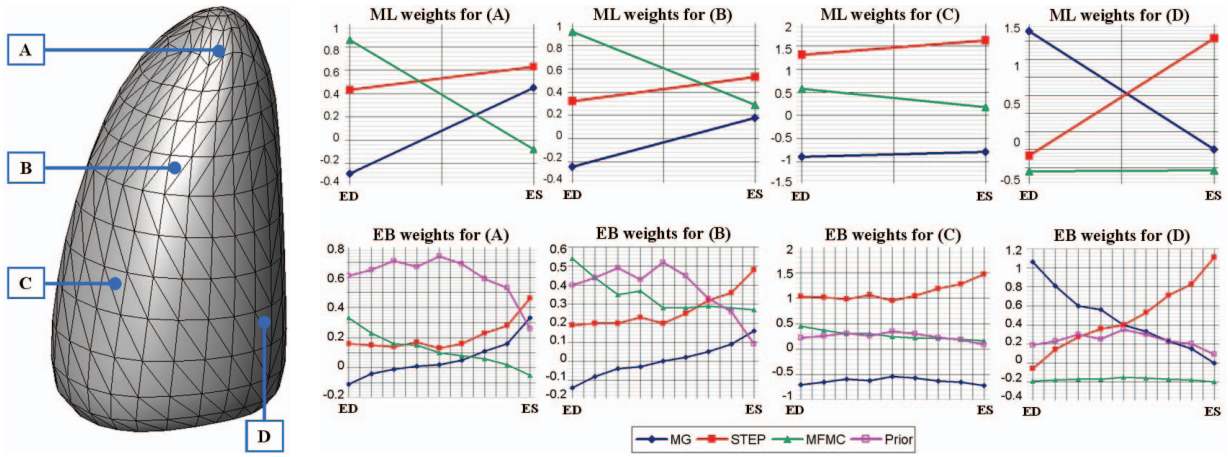


Fig. 2. Base estimator and contextual prior weights for four random surface points for the ML and EB detectors. Upper row: ML computes the optimal base detector weights for ED and ES frames, and interpolate these to all cardiac cycle. Lower row: EB multiples the ML weights with $\left(\hat{\tau}_\zeta^2 / \left(\sigma_{i,\zeta}^2 + \hat{\tau}_\zeta^2\right)\right)$ and sets the prior distribution weight as $\left(\sigma_{i,\zeta}^2 / \left(\sigma_{i,\zeta}^2 + \hat{\tau}_\zeta^2\right)\right)$ (see Equation 10). For a given endocardial surface and cardiac cycle position, sum of the weights is always 1.

and processed each frame in 6.8ms with MG, 7.5ms with STEP, 78ms with MFMC, 81ms with ML and 83ms with EB when executed on a 2.80 GHz Intel Core 2 Duo CPU.

4. CONCLUSION

We have introduced the EB approach, which finds a contextual prior capturing the probabilistic distribution of endocardial edges around a surface model, and refines ML estimations with this empirically estimated prior. The introduced method is (1) simple and efficient; computation of conceptual priors is an intuitive and computationally non-expensive task, (2) yet novel as the empirical Bayes approach has not been used for the Kalman measurements prior to our study. Results on 18 datasets demonstrate that the use of contextual information can lower the mean square estimation error as theoretically asserted by the Stein effect.

5. REFERENCES

[1] S. K. Setarehdan and John J. Soraghan, *Segmentation in echocardiographic images*, pp. 64–130, Springer-Verlag New York, Inc., New York, NY, USA, 2002.

[2] Andrew Blake and M. Isard, *Active contours: the application of techniques from graphics, vision, control theory and statistics to visual tracking of shapes in motion*, Springer-Verlag New York, Inc., Secaucus, NJ, USA, 1998.

[3] Stein Inge Rabben, Anders Herman Torp, Asbjørn Støylen, Stig Slørdahl, Knut Bjørnstad, Bjørn Olav Haugen, and Bjørn Angelsen, "Semiautomatic contour detection in ultrasound m-mode images," *Ultrasound in Medicine & Biology*, vol. 26, no. 2, pp. 287 – 296, 2000.

[4] S. Venkatesh and R. Owens, "On the classification of image features," *Pattern Recogn. Lett.*, vol. 11, no. 5, pp. 339–349, 1990.

[5] Engin Dikici and Fredrik Orderud, "Graph-cut based edge detection for Kalman filter based left ventricle tracking in 3d+ t echocardiography," in *Proceedings of Computing in Cardiology*, 2010.

[6] Engin Dikici and Fredrik Orderud, "Maximum likelihood and James-Stein edge estimators for left ventricle tracking in 3d echocardiography," in *2nd International Workshop on Machine Learning in Medical Imaging (MLMI) in conjunction with MICCAI*, 2011.

[7] Engin Dikici, Fredrik Orderud, and Hans Torp, "Best linear unbiased estimator for Kalman filter based left ventricle tracking in 3d+t echocardiography," *IEEE Workshop on Mathematical Methods in Biomedical Image Analysis (MMBIA)*, 2012.

[8] Fredrik Orderud and Stein I. Rabben, "Real-time 3d segmentation of the left ventricle using deformable subdivision surfaces," in *CVPR*, 2008.

[9] George Casella, "An introduction to empirical Bayes data analysis," *The American Statistician*, vol. 39, no. 2, pp. 83–87, 1985.

[10] Steven M. Kay, *Fundamentals of statistical signal processing: estimation theory*, Prentice-Hall, Inc., Upper Saddle River, NJ, USA, 1993.